Superoxide Production by Plant Homologues of the gp91^{phox} NADPH Oxidase. Modulation of Activity by Calcium and by Tobacco Mosaic Virus Infection[1]

Moshe Sagi[2] and Robert Fluhr*

Department of Plant Science, Weizmann Institute of Science, P.O. Box 26, Rehovot 76100, Israel

Genes encoding homologs of the gp91^{phox} subunit of the plasma membrane NADPH oxidase complex have been identified in plants and are hypothesized to be a source of reactive oxygen species during defense responses. However, the direct involvement of the gene products in superoxide (O_2^-) production has yet to be shown. A novel activity gel assay based on protein fractionation in native or sodium dodecyl sulfate (SDS)-denaturing polyacrylamide gels was developed. In native polyacrylamide gel electrophoresis, one or two major O_2^--producing formazan bands were detected in tomato (*Lycopersicum esculentum* Mill. cv Moneymaker) and tobacco (*Nicotiana tabacum* var. Samsun, NN) plasma membranes, respectively. Denaturing fractionation of tomato and tobacco plasma membrane in SDS-polyacrylamide gel electrophoresis, followed by regeneration of the in-gel activity, revealed NADPH-dependent O_2^--producing formazan bands of 106-, 103-, and 80- to 75-kD molecular masses. The SDS and native activity bands were dependent on NADPH and completely inhibited by diphenylene iodonium or CuZn- O_2^- dismutase, indicating that the formazan precipitates were due to reduction by O_2^- radicals catalyzed by an NADPH-dependent flavin containing enzyme. The source of the plasma membrane activity bands was confirmed by their cross-reaction with antibody prepared from the C terminus of the tomato gp91^{phox} homolog. Membrane extracts as well as the in-gel NADPH oxidase activities were stimulated in the presence of Ca^{2+}. In addition, the relative activity of the gp91^{phox} homolog was enhanced in the plasma membrane of tobacco mosaic virus-infected leaves. Thus, in contrast to the mammalian gp91^{phox}, the plant homolog can produce O_2^- in the absence of additional cytosolic components and is stimulated directly by Ca^{2+}.

Rapid generation of the reactive oxygen species (ROS) such as superoxide (O_2^-) and hydrogen peroxide (H_2O_2) are considered to be a component of the resistance response of plants to pathogen challenge. ROS intermediates can serve as direct protective agents by their toxicity, or by driving the cross-linking of the cell wall (Levine et al., 1994; Baker and Orlandi 1995; Lamb and Dixon, 1997). The oxidative burst can further trigger the collapse of challenged host cells at the onset of the hypersensitive response and generate apoptopic-like signals (Levine et al., 1994; Allan and Fluhr, 1997).

The kinetics and defense functions of O_2^- and H_2O_2 generation are reminiscent of the oxidative burst during activation of mammalian neutrophils. The neutrophil oxidative burst involves the reaction $O_2 + NADPH \rightarrow O_2^- + NADP^+ + H^+$ catalyzed by a plasma membrane oxidase, followed by dismutation of O_2^- to H_2O_2 (Taylor et al., 1993). The NADPH oxidase consists of two plasma membrane proteins, gp91^{phox} and p22^{phox} (phox for phagocyte oxidase), which together form heterodimeric flavocytochrome b_{-558}. The three cytosolic regulatory proteins, p40^{phox}, p47^{phox}, and p67^{phox} translocate to the plasma membrane after stimulation to form the active complex (Bokoch, 1994). For O_2^- production to occur, the participation of both membrane-associated and cytosol-derived component are required. The complex can be activated in vitro by anionic amphiphiles such as SDS (Knoller et al., 1991). In neutrophils, O_2^- can be induced in purified and relipidated cytochrome b_{-558} and by phosphatidic acid in the absence of cytosolic components (Koshkin and Pick, 1993).

A membrane-bound enzyme resembling the neutrophil NADPH oxidase likely contributes to the pathogen-induced oxidative burst in plants. O_2^- generation can be observed in pathogen-induced microsomal preparations and diphenylene iodonium (DPI), a suicide substrate inhibitor of the neutrophil NADPH oxidase, blocks the oxidative burst in plant cells (Doke, 1983; Doke and Ohashi, 1988; Levine et al., 1994). Antibodies raised against human p22^{phox}, p47^{phox}, and p67^{phox} cross-react with appropriately sized polypeptides in plant extracts (Tenhaken et al., 1995; Desikan et al., 1996; Xing et al., 1997). Molecular cloning of respiratory burst oxidase homolog (Rboh) in Arabidopsis (AtrbohA-F) and tomato (*Lycopersicum esculentum* Mill. cv Moneymaker; Lerboh1) define transcripts that can encode a protein of about 105 kD in size, with a C-terminal region that shows pronounced similarity to the 69-kD apoprotein of the

[1] This work was supported by a grant from the Israeli Ministry of Science, Culture, and Sport, within the cooperation program between the Ministry of Science and Technology of South Korea; and by the Minerva Foundation, Germany.

[2] Present address: The Institutes for Applied Research, Ben-Gurion University, P.O. Box 653, Beer Sheva 84105, Israel.

* Corresponding author; e-mail Robert.Fluhr@weizmann.ac.il; fax 972–8–9344181.

gp91^{phox}. The AtrbohA and Lerboh1 proteins have a large hydrophilic N-terminal domain that is not present in gp91^{phox}. This domain contains two calcium-binding EF hand motifs and has extended similarity to the human RanGTPase-activating protein (Keller et al., 1998; Torres et al., 1998; Amicucci et al., 1999). In plant disease response, direct activation of Rboh by calcium may be important for rapid stimulation of the oxidative burst during the hypersensitive response (Lamb and Dixon, 1997). Comparison of motifs present in the plant and animal gp91^{phox} homologs support a common mechanism for ROS production, but indicate that the regulation of oxidase activity may differ. In the current study, we developed a novel NADPH oxidase activity gel assay and show that the putative plant plasma membrane NADPH oxidase can produce O_2^-. Unlike the mamalian NADPH oxidase complex, O_2^- production proceeds in the absence of additional cytosolic components and can be directly stimulated by Ca^{2+}.

RESULTS

In-Gel Assay for NADPH Oxidase Activity

Plasma membranes and their associated proteins were isolated from tomato and tobacco (*Nicotiana tabacum* var. Samsun, NN) leaves by two-phase partitioning as described in "Materials and Methods." The efficacy of membrane partitioning was verified in immunoblots by probing with antibodies specific for the plasma membrane proteins NtCBP4 and P-ATPase (Pardo and Serrano, 1989; Arazi et al., 1999), and the 60-kD subunit of vacuolar ATPase (Ward et al., 1992). As shown in Figure 1, the vacuolar marker appears highly enriched in the lower phase, whereas the two plasma membrane markers are highly enriched in the upper phase. The membrane proteins were solubilized in 0.1% (w/v) CHAPS {3-[(3-cholamidopropyl)dimethylammonio]-1-propanesulfonic acid} detergent and then subjected to native PAGE. The fractionated proteins were examined for their ability to generate O_2^- by reduction of nitroblue tetrazolium (NBT). A single major migration band of activity was detected in native gels in tomato and two bands were detected in tobacco (Fig. 2A). The addition of DPI, a suicide substrate inhibitor of flavin containing enzymes or the addition of CuZn-SOD that dismutates O_2^-, abrogated this activity (Fig. 2A). No activity bands appeared in the gels in the absence of NADPH (data not shown). These results indicate that the blue formazan bands detected in the gels were due to NADPH-dependent NBT reduction by O_2^- radicals and that the O_2^--generating activity is the result of a flavin-dependent enzyme.

To further develop in-gel fractionation procedures, the detergent sensitivity of the plasma membrane enzyme responsible for the NADPH-dependent O_2^- production was examined. As shown in Table I, the activity was highly sensitive to the anionic amphiphile SDS but less sensitive to zwitterionic or nonionic detergents such as CHAPS and Triton X-100, respectively. This result is in contrast to that found for the mammalian NADPH oxidase complex that is activated by SDS (Knoller et al., 1991; Cross et al., 1999). Therefore, a novel denaturing gel assay was developed based on the gradual removal of SDS from the gel in the presence of 1.0% (w/v) Triton X-100 in the buffer solution and as detailed in "Materials and Methods." Under denaturing fractionation conditions, formazan-stained migration bands of 106-, 103-, and 75- to 80-kD molecular masses were detected (Fig. 2B). The higher molecular masses are consistent with the predicted mass of decoded cDNA of tomato NADPH oxidases (Amicucci et al., 1999; D.P. Puthoff and L.L. Walling, unpublished data; accession no. AF148534). To establish whether the formazan bands observed in the two gel systems were monitoring the same activity, the bands detected in native polyacrylamide gels were excised and subjected to SDS-PAGE. In this case, activity bands of similar mobility to those detected in direct SDS-denaturated gel fractionation were observed (Fig. 2C). Thus, the formazan bands detected in native PAGE result from a mixture of polypeptides or degradation of the larger polypeptide occurred during the denaturing gel procedure.

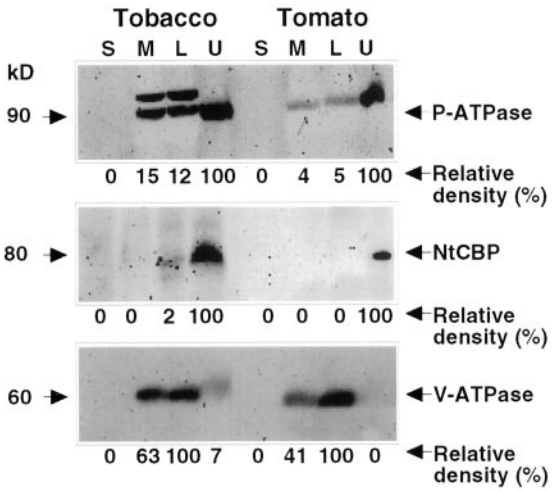

Figure 1. Western blot of tomato and tobacco membrane fractions. Supernatant (S) and microsomal membranes (M) were separated by centrifugation at 203,000*g*. The membrane pellet was then fractionated by the aqueous two-phase partitioning method into a lower phase (L) enriched for intracellular membranes and the upper phase (U) enriched with plasma membranes. Proteins (25 μg per lane) from each fraction (S, M, L, and U) were fractionated by denaturing SDS-PAGE, and immunoblotted. Blots were probed with antibodies raised against plasma membrane H-ATPase (P-ATPase), plasma membrane tobacco calmodulin-binding protein (NtCBP4), and the 60-kD subunit of vacuolar H-ATPase from oat root (V-ATPase). The relative density was established by scanning the gel as described in "Materials and Methods." In the case of the P-ATPase the lower band was scanned.

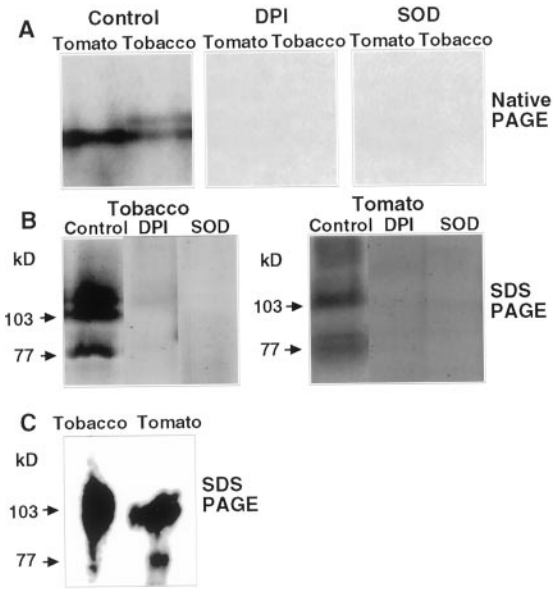

Figure 2. NADPH oxidase activity gels of tomato and tobacco leaf upper phase plasma membranes fractionated by native and denaturing SDS-PAGE. A, Tomato and tobacco membranes (50 μg) were fractionated by native PAGE and assayed for NADPH oxidase activity with or without the addition of DPI or O_2^- dismutase (SOD). B, Tomato and tobacco membranes (100 μg) were fractionated by denaturing SDS-PAGE and assayed for NADPH oxidase activity with or without the addition of DPI or SOD. C, Activity gel of refractionated NADPH oxidase activity bands. Membrane proteins of the upper phase were fractionated by native PAGE as in A. The formazan stained bands were excised, subsequently refractionated by denaturating SDS-PAGE, and an in-gel activity assay was carried out.

Immunodetection of the Plant gp91^{phox} Homolog

The molecular nature of the formazan-generating polypeptides was examined by using antisera raised against a recombinant protein fragment prepared from the C-terminal portion of the tomato gp91^{phox} homolog (EST243389). This area is highly conserved in all plant NADPH oxidases isolated to date and contains the putative NADPH-binding motifs. Tomato microsomes were fractionated by two-phase partitioning and subjected to denaturing gel analysis (Fig. 3). NADPH-dependent O_2^--producing bands were detected mainly at 103 to 106 and 75 to 80 kD. The activity was detected in both upper and lower polyethylene glycol phases but was enriched in the upper phase (central; Fig. 3). Immunoanalysis of the denaturing gel revealed immunoreactive polypeptides at masses of 103 to 106, 75 to 80, 60, and 50 kD (right; Fig. 3) that did not match to any of the major stained proteins (compare left and right, Fig. 3). The migration pattern of the immunoreactive bands at 103 to 106 and 75 to 80 kD correlated with the distribution of the activity bands but not with their relative intensity. The immunoreactive bands at 60 and 50 kD did not match the activity bands and may indicate breakdown products or be a result of nonspecific reaction. It was consistent that the major immunoreactive band detected by the antibodies was between 75 and 80 with weaker bands detected at 103 to 106 kD. In contrast, the staining of the activity bands were distributed either equally between the different masses or tended to be enriched in the 103- to 106-kD masses (compare SDS activity gel and immunoblot, Fig. 3). To understand this result, the relative activities of NADPH oxidase activity bands of the fractionated proteins were estimated by gel scanning after denaturing SDS-PAGE (Table II). The measurements revealed that only 60% of the total activity in the microsomal fraction was recovered in the upper phase fraction. The major loss was due to a reduction of 85% of the activity recovered in the 77-

Table I. *Effect of the detergents SDS, CHAPS, and Triton X-100 on tomato plasma membrane NADPH oxidase activity*[a]

Treatment	Concentration	Relative Activity
	μM and %	% ± SE
No detergent	0	100 ± 6
SDS	40 (0.0012%)	85 ± 5
	100 (0.0029%)	54 ± 4
	200 (0.0058%)	36 ± 4
	3,467 (0.1%)	0.8 ± 2
	34,674 (1%)	0
CHAPS	1,626 (0.1%)	75 ± 7
	16,263 (1%)	25 ± 5
	32,526 (2%)	21 ± 7
Triton X-100	15,480 (1%)	33 ± 5

[a] Membrane fractions were obtained from the upper phase of aqueous two-phase partitioning. The superoxide production (reduction of 2, 3-bis [2-methoxy-4-nitro-5-sulfophenyl 2H-tetrazolium-5-carboxanilicle [XTT]]) was quantified as described in "Materials and Methods." The activity is expressed as percentage of control values without detergents (100% = 0.395 ± 0.027 of XTT formazan absorbance at 470 0.6 h^{-1} 3 μg^{-1} plasma membrane protein). Means and SE are calculated for two to three independent plasma membrane preparations.

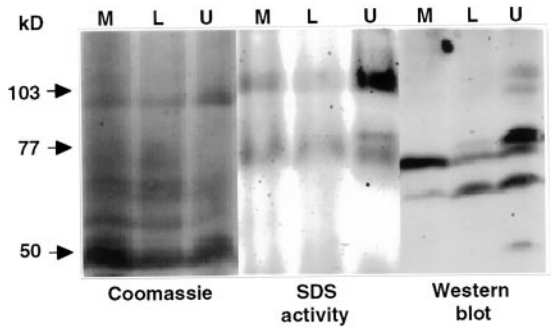

Figure 3. Activity gel assay and immunodetection of NADPH oxidase in tomato plasma membranes. Membranes (M) were fractionated by the aqueous two-phase partitioning method into a lower phase (L) enriched with intracellular membranes and an upper phase (U) enriched with plasma membranes. Proteins from each fraction (60 μg per lane) were fractionated by denaturating SDS-PAGE and immunoblotted with antisera against the C-terminal portion of the tomato Rboh (western blot), or stained for NADPH activity (SDS activity) or Coomassie Blue (Coomassie) as described in "Materials and Methods."

Table II. *Relative activity of NADPH oxidase activity bands (103–106 and 75–80 kD) in the fractionated supernatant and membrane proteins in the SDS in-gel assay*

Fraction	Molecular	Soluble Protein	Relative Activity	Total Relative Activity (Soluble Protein × Relative Activity)
	kD	*μ fraction*$^{-1}$		
Supernatant (203,000 g)	103–106	813,000	0	0
	77–80		0	0
Pellet (203,000 g)	103–106	8,950	4	35,800
	77–80		4	35,800
Lower phase	103–106	350	1	350
	77–80		3	1,050
Upper phase	103–106	370	100	37,000
	77–80		15	5,550

[a] Extracts from 150 g of tomato leaves were centrifuged at 10,000*g*. The supernatant was subjected to centrifugation at 203,000*g* to yield the microsomal fraction. Lower and upper phases were partitioned from the microsomal fraction by the two-phase system and fractionated by SDS-PAGE as described in "Materials and Methods." The activity gels were scanned and the results presented in arbitrary relative units.

to 80-kD fraction (Table II), indicating that the activity in this fraction is labile. Inactivation of this class of polypeptides is consistent with the discrepancy between the results of the immunoblot and gel activity assays.

Activation of O_2^- Activity by Calcium Ions

The plant NADPH oxidase homologs contain two putative Ca^{2+}-binding EF hand motifs that were shown to bind calcium $^{45}Ca^{2+}$ (Keller et al., 1998). The possible interaction of NADPH oxidase and Ca^{2+} was examined in two-phase fractionated leaf extracts of tomato and tobacco. NADPH oxidase showed high basal activity without Ca^{2+} added to the reaction medium (Fig. 4). The addition of 10 mM EGTA did not influence the basal level of O_2^- production. The activity was further induced by the addition of Ca^{2+} starting from 50 μM to a maximum 2-fold enhancement at millimolar levels of Ca^{2+} (Fig. 4, insert). The induction by calcium was blocked by the addition of EDTA (Fig. 4). Gel-fractionated polypeptides were also examined for sensitivity to calcium. Calcium-dependent enhancement of intensity of the formazan band formation was detected in native and denaturing gel systems showing approximately 3- and 1.5-fold induction, respectively (Fig. 5). In the denaturing system, both masses of 103 and 77 kD were detected and showed calcium sensitivity. Thus, if the calcium enhancement of activity is due to binding by the EF hands, the processed form of the 77-kD mass likely retains this motif.

Activation of O_2^- Activity in Extracts of Tobacco Mosaic Virus (TMV)-Infected Plants

TMV can replicate systemically in tobacco plants containing the N-type TMV resistance gene when the inoculated plants are maintained at 30°C. After transfer to a lower temperature, a synchronized systemic hypersensitive response rapidly ensues that is accompanied within 1 h by an oxidative phase I burst (Doke and Ohashi, 1988; A. Allan, M. Lapidot, and R. Fluhr, personal communication). NADPH oxidase activity was examined in systemically infected leaves maintained at 30°C for 36 h and then transferred to 20°C for 1 h before measurements. Under these conditions, leaf discs showed more than 3-fold higher O_2^- production in TMV inoculated leaves than noninoculated leaves (Fig. 6A). NADPH oxidase activity

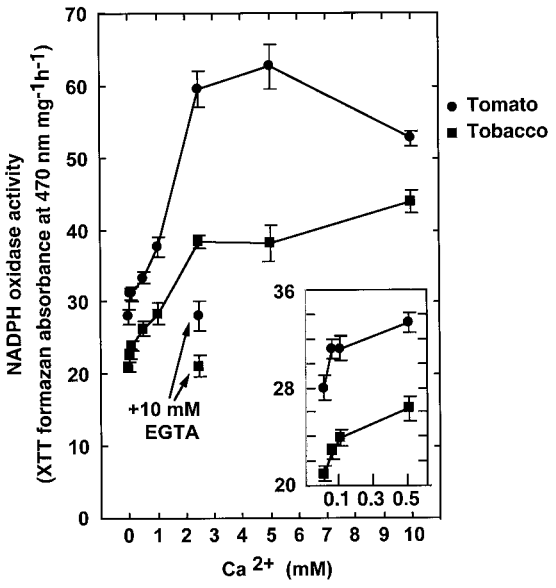

Figure 4. NADPH oxidase activity in isolated tomato and tobacco membranes. NADPH activity was assayed in membranes of the upper phase of aqueous two-phase partitioned membranes. XTT reduction by O_2^- is shown corrected for reduction in the presence of SOD (50 units mL^{-1}). Where indicated 10 mM EGTA was added. Data are mean ± SE of four repeats and represent one of three different experiments that yielded essentially identical results.

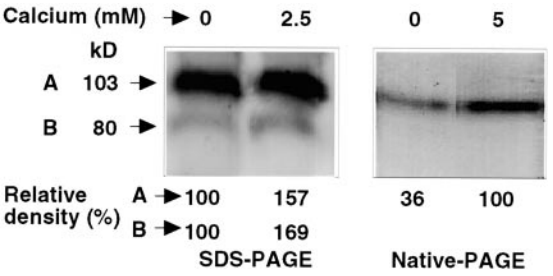

Figure 5. In-gel assay for NADPH oxidase activity in tomato membranes as affected by Ca^{+2} in the reaction medium. Plasma membrane proteins (60 μg per lane) were fractionated by denaturating SDS-PAGE or native PAGE and stained for activity in the presence or absence of Ca^{+2} in the reaction buffer.

was next examined in fractionated plasma membranes. Membrane fractions from inoculated leaves contain many TMV particles (Doke and Ohashi, 1988); therefore, NADPH oxidase activities are shown compared with each other on a leaf fresh weight basis (Fig. 6, A and B). O_2^--generating activity in plasma membranes were found to be more than 3-fold higher in TMV-inoculated compared with noninoculated leaves (Fig. 6A). In-gel denaturing and native gel assay of the membrane fractions revealed over 1.5- and 2.5-fold enhancement of O_2^- production, respectively, in fractionated extracts of inoculated compared with control leaves (Fig. 6B). The increase in activity may be due to de novo biosynthesis or result from intrinsic activation of Rboh.

DISCUSSION

Multigene families encoding potential NADPH oxidase homologs have been described in Arabidopsis and tomato (Keller et al., 1998; Torres et al., 1998; Amicucci et al., 1999; D.P. Puthoff and L.L. Walling, unpublished data; accession no. AF148534). As shown here, the Rboh gene products reduce NBT and can be inhibited by DPI and SOD (Fig. 2), indicating that they produce O_2^-s in a NADPH and flavin-dependent manner. The results are consistent with the evidence that O_2^- production in vivo is associated with a flavin containing NADPH oxidase-like activity (Auh and Murphy, 1995; Murphy and Auh, 1996; Gestelen et al., 1997; Lamb and Dixon, 1997).

Cytosolic components of the mammalian phagocyte NADPH oxidase, including $p67^{phox}$, $p47^{phox}$, and Rac2, are translocated to the plasma membrane upon cell activation where they interact with a membrane-bound cytochrome. (Dorseuil et al., 1995). Thus, activation of the neutrophil NADPH oxidase is completely dependent on the participation of both a membrane-bound flavocytochrome b_{-558} and cytosol-derived components (Knoller et al., 1991; Babior 1999; Cross et al., 1999). In contrast, plant membrane extracts can catalyze the production of O_2^- after being subjected to both native PAGE (in the presence or absence of the detergent CHAPS) or after denaturing SDS-PAGE. This indicates that the plant plasma membrane NADPH oxidase can produce O_2^- in the absence of additional cytosolic components (Figs. 2–4 and 6). The result is consistent with the failure of attempts to clone plant $p40^{phox}$, $p47^{phox}$, and $p67^{phox}$ homologs (Tenhaken and Rübel, 1999) or find significant evidence for their existence in the completed Arabidopsis genome (data not shown; see "Materials and Methods"). Additional dissimilarities between animal and plant enzymes are indicated by the sensitivity to detergents. The mammalian NADPH oxidase complex is activated by SDS, whereas the plant plasma membrane NADPH oxidase activity is completely inhibited (Table I; Bromberg and Pick, 1985; Knoller et al., 1991; Cross et al., 1999).

The relatively high basal Rboh activity detected in vitro may be a reflection of the O_2^- production that is detected in vivo in non-treated plants (Doke and Ohashi, 1988; Ogawa et al., 1997; Able et al., 1998). The further increase in Rboh activity in vivo during the pathogenesis response may be due to changes in substrate (NADPH) availability, modulation of Rboh by cytoplasmic factors, or down-regulation of the cellular ROS scavenging capability. In the latter case,

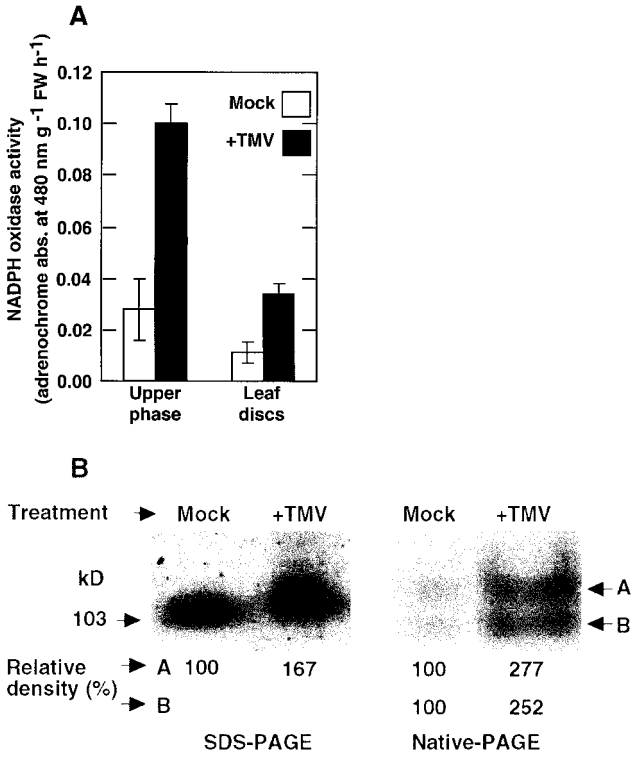

Figure 6. Plasma membrane NADPH oxidase activities and O_2^- production in leaf discs and membranes isolated from TMV-inoculated and control tobacco leaves. A, NADPH oxidase in isolated membranes (left) and extracellular O_2^- generating activity of leaf discs (right). In each measurement, amounts measured are based on equal fresh weight as described in "Results." B, In-gel assay for NADPH oxidase activity in plasma membranes isolated from control and TMV-infected leaves. In each measurement, amounts loaded on the gels are based on equal fresh weight as described in "Results."

the basal rate of activity would be rapidly modulated by recruitment of ROS detoxifying pathways as has recently been suggested (Mittler et al., 1999a, 1999b).

Our results revealed that formazan activity bands are present at masses of the expected size of 106 and 103 kD as well as 80 to 75 kD (Figs. 2–4). The origin of the plasma membrane activity bands was confirmed by their cross-reaction with antibody prepared from the C terminus of the tomato gp91^{phox} homolog, Wfil (Fig. 4). Similar to Arabidopsis, it is likely that tobacco and tomato have multiple genes encoding gp91^{phox}-like proteins, and that the activity measured represents the sum total of several enzymes. The putative decoded polypeptide size of Arabidopsis and tomato gp91^{phox}-like transcripts predict polypeptide sizes in a range between 94- and 112-kD masses (Keller et al., 1998; Torres et al., 1998; Amicucci et al., 1999; D.P. Puthoff and L.L. Walling, unpublished data; accession no. AF148534). Antisera raised against a conserved peptide located near the C terminus of Rice RbohA protein were shown to react with a 97-kD protein in rice cell extracts and a 105-kD polypeptide in Arabidopsis cell extracts (Keller et al., 1998). Additional immunoreactive proteins of 60 to 80 kD that appeared in Arabidopsis plasma membrane fraction were assumed to reflect partial degradation of AtRbohA (Keller et al., 1998). Scanning the complete Arabidopsis genome with BLAST and PSI-BLAST algorithims did not reveal significant homology to predicted genes of shorter length (E values < -145 for the full-length gp91^{phox} family compared with E = -13 and larger for the nearest homologs of different gene sizes; see "Materials and Methods").

Thus, the variability in polypeptide size detected here could be the result of a Rboh splicing variants or alternatively arise from cellular posttranscriptional proteolytic processes or from isolation artifacts. In any event, a polypeptide above 75 kD in mass that was truncated in the N terminus would still retain the two EF hand motifs, six putative membrane spans, FAD-isoalloxazine, and NAD/P-Rib and NAD/P-adenine motifs, and thus can be assumed to retain enzymatic activity as is shown here. Based on the intensity of immunoreactive bands, a majority of the gene product appears to be in the processed 75- to 80-kD size after fractionation under denaturing conditions, yet most of the in-gel activity is detected in the higher molecular mass migrating bands. Thus, the N terminus may play a role in regulatory activation. In this respect, it remains to be seen whether this region could mediate the involvement of the small GTP-binding protein Rac that was shown to be involved in activating ROS production (Kawasaki et al., 1999; Hassanain et al., 2000; Park et al., 2000).

A 2- to 3-fold increase in O_2^- production was detected in membrane extracts upon addition of Ca^{2+} (Figs. 4 and 5). This compares with approximately 3-fold induction in O_2^- produced by leaf discs in response to viral infection (Fig. 6 and Doke and Ohashi, 1988). Thus, direct regulation by calcium may be responsible for at least part of the induction of the plant oxidative burst. In neutrophils, phosphorylation of p47^{phox} by protein kinase C contributes to Ca^{2+}-dependent NADPH oxidase activation (Dusi et al., 1993; Bokoch, 1994; Korchak et al., 1998). The existence of a Ca^{2+}-dependent O_2^--generating system was previously shown in microsomes isolated from TMV-inoculated tobacco leaf using a cytochrome C assay (Doke and Ohashi, 1988). Putative p47^{phox}-binding sites are conserved in plant gp91^{phox} homologs; however, such proteins have yet to be detected in plants (Tenhaken and Rübel, 1999). Ca^{2+}-dependent protein phosphorylation may contribute to the activation of NADPH oxidase in plants. However, the presence of the highly conserved EF hand motifs in all known Rboh putative proteins and the strong Ca^{2+} binding by a synthetic version of RbohA EF hand motifs provides a potential direct mechanism for regulation by Ca^{2+} (Keller et al., 1998; Torres et al., 1998). Substantial in-gel Ca^{2+} sensitivity could be demonstrated in isolated polypeptides from tobacco and tomato. The plasma membrane NADPH oxidase showed a basal rate of O_2^- generation in the presence of 10 mM EGTA (Fig. 4). Significant increases in NADPH oxidase activity could be detected between 50 μM and 10 mM $CaCl_2$ (Figs. 4 and 5). Thus, in vitro the plant plasma membrane NADPH oxidase, unlike neutrophil gp91^{phox}, can be regulated directly by Ca^{2+}.

The Ca^{2+} levels that were found to modulate NADPH oxidase activity may appear to be relatively high for proteins involved in Ca^{2+}-regulated cytosolic processes. For example, proteins that contain EF hand motifs show high affinity to Ca^{2+} (10^{-9}–10^{-4}; Ikura, 1996). However, EF hand-containing proteins that are localized to the secretory pathway possess low Ca^{2+} affinity with dissociation constants between 10^{-4} and 10^{-3} M (Meldolesi and Pozzan, 1998; Vorum et al., 1998; Honore and Vorum, 2000). Thus, Ca^{2+} levels shown to induce NADPH oxidase are consistent with low affinity EF hands and may reflect the elevated concentrations of Ca^{2+} released and sequestered around membrane-bound plant NADPH oxidases during pathogenesis.

O_2^- production levels in vivo can be induced by elicitors, mechanical factors, or during pathogenesis (Auh and Murphy, 1995; Pugin et al., 1997; Minibayeva et al., 1998; Park et al., 1998). The regulation of this activity may be due to stress-induced interaction of the Rboh with cytosolic factors, increased calcium levels or modification of the polypeptide quantity or activity. SDS and native in-gel assay for NADPH oxidase activity conducted in systemically TMV-infected tobacco leaves revealed an increase in O_2^- production that paralleled the enhancement revealed in vivo (Fig. 6). The small differences in the degree of O_2^- enhancement between the isolated

membrane and in-gel assay may reflect experimental limitations or be due to the lack of additional regulatory components that are lost during native and SDS-PAGE. Our methods cannot differentiate between the possibility that the increase in O_2^- production is due to de novo biosynthesis or intrinsic modification of the tobacco Rboh. In either case, they show that the early burst in ROS activity is probably via NADPH oxidase-dependent O_2^- enhancement and that suppression of ROS scavenging mechanisms does not play a role in early ROS bursts. The experimental systems described here should facilitate elucidating the biological role of the NADPH oxidase plant homologs and their regulation.

MATERIALS AND METHODS

Plant Material

Tomato (*Lycopersicum esculentum* Mill. cv Moneymaker) and tobacco (*Nicotiana tabacum* var. Samsun, NN) were grown in pots filled with peat and vermiculite (4:1, v/v) mixture containing slow-release High N multicote 4 with microelements (Haifa Chemicals Ltd, Haifa, Israel; 0.3% [w/w]). Greenhouse average temperatures during the growth period fluctuated from 18°C to 25°C. Midday photosynthetic photon flux density in the greenhouse was 300 to 500 μmol m^{-2} s^{-1}.

Expression of Recombinant Proteins and Antibody Preparation

A 653-bp-long *Eco*RI fragment from a tomato cDNA clone (EST243389) was fused to the glutathione S-transferase protein from *Schistosoma japanicum*, using the pGEX expression vector (Pharmacia, Piscataway, NJ). The resulting fusion protein contained 214 C-terminal amino acids of the tomato NADPH homolog, Wfi1 (D.P. Puthoff and L.L. Walling, unpublished data; accession no. AF148534) and was used to immunize guinea pigs at 2-week intervals. The primary antibodies were diluted 7,500-fold in the immunoassay.

Preparation and Fractionation of Membranes

Fully expanded leaves of tomato and tobacco samples were obtained from 40- and 75-d-old plants, respectively. Samples were ground using a pestle and mortar in a buffer (1.5 mL g^{-1} fresh weight) containing 0.25 M Suc, 50 mM HEPES [4-(2-hydroxyethyl)-1-piperazineethanesulfonic acid]-KOH (pH 7.2), 3 mM EDTA, 1 mM dithiothreitol (DTT), 0.6% (w/v) polyvinylpyrrolidone, 3.6 mM L-Cys, 0.1 mM $MgCl_2$, and a cocktail of protease inhibitors including phenylmethylsulfonyl fluoride (2 mM), aprotinin (10 μg ml^{-1}), leupeptin (10 μg ml^{-1}), and pepstatin (10 μg ml^{-1}). The homogenate was filtered through two layers of Miracloth (Calbiochem, La Jolla, CA), and the resulting filtrate was centrifuged at 10,000*g* for 45 min. Microsomal membranes were pelleted from the supernatant by centrifugation at 203,000*g* for 60 min.

For aqueous two-phase partitioning, the microsomes from tomato and tobacco leaves (150 g fresh weight) were gently resuspended in 0.33 M Suc and 5 mM potassium phosphate (pH 7.8), 3 mM KCl, and protease inhibitors. The suspension was then fractionated by the aqueous two-phase partitioning method according to the batch procedure as described (Larsson et al., 1987). Phase separations were carried out in a series of 10-g phase systems with a final composition of 6.2% (w/w) dextran T500, 6.2% (w/w) polyethylene glycol 3350, 0.33 M Suc, and 5 mM potassium phosphate (pH 7.8), 3 mM KCl, and protease inhibitors. Three successive rounds of partitioning yielded final upper phases (U_3 and $U_{3'}$) and lower phase (L_3). The combined upper phase was enriched in plasma membranes vesicles and the lower phase contained intracellular membranes. The final upper and lower phases were diluted 5- and 10-fold, respectively, in ice-cold Tris-HCl dilution buffer (10 mM, pH 7.4) containing 0.25 M Suc, 3 mM EDTA, 1 mM DTT, 3.6 mM L-Cys, 0.1 mM MgCl, and the protease inhibitors. The fractions were centrifuged at 203,000*g* for 60 min. The pellets were then resuspended in Tris-HCl dilution buffer and used immediately for further analysis. All procedures were carried out at 4°C.

Gel Electrophoresis

Membrane fractions or supernatant were subjected to SDS-PAGE in a Bio-Rad Mini-Protean II or Protean II (20-cm plates) slab cell (Bio-Rad, Richmond, CA), with the discontinuous buffer system (Laemmli, 1970) in 7.5% (w/v) polyacrylamide separating gels and 4% (w/v) stacking gels. Samples were incubated at 45°C for 30 min in sample buffer with a final concentration of 47 mM Tris-HCl (pH 7.8), 2% (w/v) SDS, 7.5% (v/v) glycerol, and 40 mM DTT as the thiol-reducing agent (Bischoff et al., 1998), and 0.002% (w/v) bromphenol blue. The supernatants were centrifuged at 15,000*g* for 2.5 min before loading. Native PAGE was carried out as above in 7.5% (w/v) polyacrylamide separating gel and 4% (w/v) stacking gels with or without 0.1% (w/v) CHAPS. Before fractionation, the samples were maintained for 30 min at 45°C in Tris-HCl (pH 7.8) buffer with or without 0.1% (w/v) CHAPS.

NADPH Oxidase In-Gel Assays and Regeneration of Activity Following SDS-PAGE

The NADPH-dependent O_2^--producing capabilities of membrane fractions were assayed in gels by a modified NBT reduction method (Lopez-Huertas et al., 1999). Gels were incubated in the dark for 20 min in a reaction mixture solution containing 50 mM Tris-HCl buffer (pH 7.4), 0.2 mM NBT, 0.1 mM $MgCl_2$, and 1 mM $CaCl_2$. NADPH (0.2 mM) was added and the appearance of blue formazan bands were monitored. Where indicated, DPI (50 μM) or CuZn-SOD (50 units mL^{-1}) were added as controls. The reaction was stopped by immersion of the gels in distilled water. The gels were scanned in a Duoscan T1200 Scanner (Agfa, Mortsel, Belgium) and quantified by the NIH Image Software (Version 1.6). Where indicated the activity bands

detected after native PAGE were excised and crushed in the presence of the sample buffer and incubated at 45°C for 30 min and subjected to refractionation in denaturing SDS-PAGE.

Regeneration of active proteins after denaturing PAGE was performed by removal of SDS followed by enzyme activity restoration. The denaturing SDS gel was treated by shaking the gel for 90 min in 10 mM Tris-HCl buffer (pH 7.8) solution (65 mL buffer per mL of gel) containing 2% (w/v) EDTA and 1.0% (w/v) Triton X-100 (Bischoff et al., 1998, and references therein). Gels were then treated by shaking for 45 min in 20 mM Tris-HCl buffer (pH 7.4) solution (65 mL buffer per mL gel) containing 25 μM FAD, 1 mM DTT, 0.1 mM $MgCl_2$, and 1 mM $CaCl_2$. Removal of SDS and activity restoration procedures were performed at 25°C.

Calcium-Dependent O_2^- Production

NADPH oxidase was assayed in membranes by a modified assay based on reduction of XTT by O_2^- radicals (Able et al., 1998). The assay reaction medium contained 10 μg upper phase proteins, 0.3 mM XTT, and 0.18 mM NADPH in 1 mL 50 mM Tris-HCl buffer (pH 7.4) with varying concentrations of $CaCl_2$ (0–10 mM) or 10 mM EGTA. The reaction was initiated with the addition of NADPH. XTT reduction was determined at 470 nm in the presence and absence of 50 units CuZn-SOD.

Western Blot and Coomassie Staining of Proteins

Membrane proteins separated by SDS-PAGE were blotted to polyvinylidene difluoride membranes (Immun-Blot Membranes, Bio-Rad) and subjected to either immunodetection with antibodies against Rboh or antibodies against specific membrane components using the ECL detection system (Amersham Corp. Uppsala) according to the manufacture's instructions. Purity of membranes was analyzed with specific antibodies to NtCBP4 (gift of Hillel Fromm, Weizmann Institute, Rehovot, Israel; Arazi et al., 1999), the 60-kD subunit of vacular H^+-ATPase from oat roots (V-ATPase; gift of Heven Sze, University of Maryland, College Park; Ward et al., 1992), and plasma membrane H^+-ATPase (P-ATPase; gift of Ramon Serrano, Universidad Politecnica de Valencia, Camino de Verra s/n, Valencia Spain; Pardo and Serrano, 1989).

Inoculation with TMV and Assay of O_2^--Generating Activity and NADPH Oxidase Activity

Tobacco plants containing four to six fully expended leaves were decapitated. Plants were inoculated with equal amounts of TMV strain U1 in 5 mM potassium phosphate buffer (pH 7) or mock infected with 5 mM phosphate buffer. The plants were maintained at 30°C for 36 h before transfer to 20°C.

Leaf discs of 2-mm diameter were removed from the treated plants, weighed, and immersed in 50 mM Tris-HCl buffer (pH 7.8) for 60 min and then transferred to 2 mL of a reaction mixture consisting of 1 mM epinephrine in 2 mL of 50 mM Tris-HCl buffer (pH 7.8), with 1 mM KCN. The O_2^--generating activity of leaf discs was assayed spectrophotometrically by measuring the oxidation of epinephrine to adrenochrome at 480 nm (Mirsa and Fridovich, 1972). Plasma membranes were isolated from TMV-inoculated and -noninoculated uniform leaves (50 g of each treatment) as described above. NADPH oxidase activities of the membrane fractions were assayed by measuring the oxidation of epinephrine to adrenochrome at 480 nm. The assay reaction medium contained 10 μL upper phase preparation, 1 mM epinephrine, and 0.18 mM NADPH in 1 mL 50 mM Tris-HCl buffer (pH 7.8). The reaction started with the addition of NADPH and the reading of adrenochrome produced by the O_2^- radicals was corrected for background production in the presence of 50 units mL^{-1} CuZn-SOD.

Database Searches

Sequence homology analysis was carried out using allogorithims of BLAST and PSI-BLAST (http://www.ncbi.nlm.nih.gov/BLAST/) and the data bases at NCBI and Munich Information Center for Protein Sequences Arabidopsis group (http://mips.gsf.de/proj/thal/db/index.html).

Received December 29, 2000; returned for revision March 11, 2001; accepted April 20, 2001.

LITERATURE CITED

Able AJ, Guest DI, Sutherland MW (1998) Use of a new tetrazolium-based assay to study the production of superoxide radicals by tobacco cell cultures challenged with avirulent zoospores of *Phytophthora parasitica* var *nicotianae.* Plant Physiol **117:** 491–499

Allan AC, Fluhr R (1997) Two distinct sources of elicitated reactive oxygen species in tobacco epidermal cells. Plant Cell **9:** 1559–1572

Amicucci E, Gaschler K, Ward JM (1999) NADPH oxidase genes from tomato (*Lycopersicon esculentum*) and Curly-leaf pondweed. Plant Biol **1:** 524–528

Arazi T, Sunkar R, Kaplan B, Fromm H (1999) A tobacco plasma membrane calmodulin-binding transporter confers Ni^{2+} tolerance and Pb^{2+} hypersensitivity in transgenic plants. Plant J **20:** 171–182

Auh CK, Murphy TM (1995) Plasma membrane redox enzyme is involved in the synthesis of O_2^- and H_2O_2 by *Phytophthora* elicitor-stimulated rose cells. Plant Physiol **107:** 1241–1247

Babior BM (1999) NADPH oxidase: an update. Blood **93:** 1464–1476

Baker CJ, Orlandi EW (1995) Active oxygen in plant pathogenesis. Annu Rev Phytopathol **33:** 299–321

Bischoff KM, Shi L, Kennelly PJ (1998) The detection of enzyme activity following sodium dodecyl sulfate polyacrylamide gel electrophoresis. Anal Biochem **260:** 1–17

Bokoch GM (1994) Regulation of the human neutrophil NADPH oxidase by the Rac GTP-binding proteins. Curr Opin Cell Biol **6:** 212–218

Bromberg Y, Pick E (1985) Activation of NADPH-dependent superoxide production in a cell free system by sodium dodecyl sulfate. J Biol Chem **260:** 13539–13545

Cross AR, Erickson RW, Ellis BA, Curnutte JT (1999) Spontaneous activation of NADPH oxidase in a cell-free system: unexpected multiple effects of magnesium ion concentrations. Biochem J **338:** 229–233

Desikan R, Hancock JT, Coffey MJ, Neill SJ (1996) Generation of active oxygen in elicited cells of *Arabidopsis thaliana* is mediated by a NADPH oxidase-like enzyme. FEBS Lett **382:** 213–217

Doke N (1983) Involvement of superoxide anion generation in the hypersensitive response of potato tuber tissues to infection with an incompatible race of *Phytophthora infestans* and to the hyphal wall components. Physiol Plant Pathol **23:** 345–357

Doke N, Ohashi Y (1988) Involvement of an O_2^- generating system in the induction of necrotic lesions on tobacco leaves infected with tobacco mosaic virus. Physiol Mol Plant Pathol **32:** 163–175

Dorseuil O, Quinn MT, Bokoch GM (1995) Disassociation of Rac translocation from $p47^{phox}/p67^{phox}$ movement in human neutrophils by tyrosine kinase inhibitors. J Leukoc Biol **58:** 108–113

Dusi S, Dellabianca V, Grzeskowiak M, Rossi F (1993) Relationship between phosphorylation and translocation of the plasma-membrane of $p47^{phox}$ and $p67^{phox}$ and activation of the NADPH oxidase in normal and Ca^{2+}-deplated human meutrophils. Biochem J **290:** 173–178

Gestelen PV, Asrad H, Caubergs RJ (1997) Solubilization and separation of a plant plasma membrane NADPH-O_2^- synthase from other NAD(P) H oxidoreductases. Plant Physiol **115:** 543–550

Hassanain HH, Sharma YK, Moldovan L, Khramtsov V, Berliner LJ, Duvick JP, Goldshmidt-Clermont PJ (2000) Plant rac proteins induce superoxide production in mammalian cells. Biochem Biophys Research Commun **272:** 783–788

Honore B, Vorum H (2000) The CREC family, a novel family of multiple EF-hand, low affinity Ca_2^+-binding proteins localized to the secretory pathway of mammalian cells. FEBS Lett **466:** 11–18

Ikura M (1996) Calcium binding and conformational response in EF-hand proteins. Trends Biochem Sci **21:** 14–17

Kawasaki T, Henmi K, Ono E, Hatakeyama S, Iwano M, Satoh H, Shimamoto K (1999) The small GTP-binding protein Rac is a regulator of cell death in plants. Proc Natl Acad Sci USA **96:** 10922–10926

Keller T, Damude HG, Werner D, Doerner P, Dixon RA, Lamb C (1998) A plant homolog of the neutrophil NADPH oxidase $gp91^{phox}$ subunit gene encodes a plasma membrane protein with Ca^{2+} binding motifs. Plant Cell **10:** 255–266

Knoller S, Shpungin S, Pick E (1991) The membrane-associated component of the amphiphile-activated, cytosol-dependent superoxide-forming NADPH oxidase of macrophages is identical to $cytochrome_{b559}$. J Biol Chem **266:** 2795–2804

Korchak HM, Rossi MW, Kilpatrick LE (1998) Selective role of β-protein kinase C in signaling for O_2^- generation but not degranulation or adherence in differentiated HL60 cells. J Biol Chem **273:** 27292–27299

Koshkin V, Pick E (1993) Generation of superoxide by purified and relipidated cytochrome b559 in the absence of cytosolic activators. FEBS Lett **327:** 57–62

Laemmli UK (1970) Cleavage and structural proteins during the assembly of the head of bacteriophage T4. Nature **227:** 680–685

Lamb C, Dixon RA (1997) The oxidative burst in plant disease resistance. Annu Rev Plant Physiol Plant Mol Biol **48:** 251–275

Larsson C, Widell S, Kjellbom P (1987) Preparation of high-purity plasma membranes. Methods Enzymol **148:** 558–568

Levine A, Tenhaken R, Dixon R, Lamb C (1994) H_2O_2 from the oxidative burst orchestrates the plant hypersensitive disease resistance response. Cell **79:** 583–593

Lopez-Huertas E, Corpas JF, Sandalio ML, del Rio AL (1999). Characterization of membrane polypeptides from pea leaf peroxisomes involved in superoxide radical generation. Biochem J **337:** 531–536

Meldolesi J, Pozzan T (1998) The endoplasmic reticulum Ca_2^+ store: a view from the lumen. Trends Biochem Sci **23:** 10–14

Minibayeva FV, Kolesnikov OP, Gordon LK (1998) Contribution of a plasma membrane redox system to the superoxide production by wheat root cells. Protoplasma **205:** 101–106

Mirsa HR, Fridovich I (1972) The univalent reduction of oxygen by reduced flavins and quinones. J Biol Chem **247:** 188–192

Mittler R, Lam E, Shulaev V, Cohen M (1999a) Signal controlling the expression of cytosolic ascorbate peroxidase during pathogen-induced programmed cell death in tobacco. Plant Mol Biol **39:** 1025–1035

Mittler R, Herr EH, Orvar BL, Camp WV, Wilekens H, Inzé D, Ellis BE (1999b) Transgenic tobacco plants with reduced capability to detoxify reactive oxygen intermediates are hyperresponsive to pathogen infection. Proc Natl Acad Sci USA **95:** 5818–5823

Murphy TM, Auh CK (1996) The superoxide synthases of plasma membrane preparations from cultured rose cells. Plant Physiol **110:** 621–629

Ogawa K, Kanematsu S, Asada K (1997) Generation of superoxide anion and localization of CuZn-superoxide dismutase in the vascular tissue of spinach hypocotyls: their association with lignification. Plant Cell Physiol **38:** 1118–1126

Pardo JM, Serrano R (1989) Structure of plasma membrane H^+-ATPase gene from the plant *Arabidopsis thaliana*. J Biol Chem **264:** 8557–8562

Park H, Miura Y, Kawakita K, Yoshioka H, Doke N (1998) Physiological mechanisms of a sub-systemic oxidative burst triggered by elicitor-induced local oxidative burst in potato tuber slices. Plant Cell Physiol **39:** 1218–1225

Park J, Choi HJ, Lee S, Lee T, Yang Z, Lee Y (2000) Rac-related GTP-binding protein in elicitor-induced reactive oxygen generation by suspension-cultured soybean cells. Plant Physiol **124:** 725–732

Pugin A, Frachisse JM, Tavernier E, Bligny R, Gout E, Douce R, Guern J (1997) Early events induced by elicitor cryptogein in tobacco cells: involvement of plasma mem-

brane NADPH oxidase and activation of glycolysis and the pentose phosphate pathway. Plant Cell **9:** 2077–2091

Taylor WR, Jones DT, Segal AW (1993) A structural model for the nucleotide binding domains of the flavocytochrome b-245 β-chain. Protein Sci **2:** 1675–1685

Tenhaken R, Levine A, Brisson LF, Dixon RA, Lamb C (1995) Function of the oxidative burst in hypersensitive disease resistance. Proc Natl Acad Sci USA **92:** 4158–4163

Tenhaken R, Rübel C (1999) Cloning of putative subunits of the soybean plasna membrane NADPH oxidase involved in the oxidative burst by antibody expression screening. Protoplasma **205:** 21–28

Torres MA, Onouchi H, Hamada S, Machida C, Hammond-Kossack KE, Jones JDG (1998) Six *Arabidopsis thaliana* homologues of the human respiratory burst oxidase (*gp91*^{phox}). Plant J **14:** 365–370

Vorum H, Liu X, Madsen P, Rasmussen HH, Honore B (1998) Molecular cloning of a cDNA encoding human calumenin, expression in *Escherichia coli* and analysis of its Ca_2^+-binding activity. Biochim Biophys Acta **1386:** 121–131

Ward J, Reinders A, Hsu H, Sze H (1992) Dissociation and reassembly of the vacoular H^+-ATPase complex from oat roots. Plant Physiol **99:** 161–169

Xing T, Higgins VJ, Blumwald E (1997) Race-specific elicitors of *Cladosporium fulvum* promote translocation of cytosolic components of NADPH oxidase to the plasma membrane of tomato cells. Plant Cell **9:** 249–259